Effects of human-induced land degradation on water and carbon fluxes in two different Brazilian dryland soil covers

Michele L. de Oliveira [a], Carlos A.C. dos Santos [a,b,*], Gabriel de Oliveira [c], Aldrin M. Perez-Marin [d], Celso A.G. Santos [e]

[a] Graduate Program in Engineering and Natural Resources Management, Federal University of Campina Grande, Campina Grande, Paraíba 58109-970, Brazil
[b] Academic Unit of Atmospheric Sciences, Federal University of Campina Grande, Campina Grande, Paraíba 58109-970, Brazil
[c] Department of Earth Sciences, University of South Alabama, Mobile, AL 36688, USA
[d] National Institute of Semi-Arid, Campina Grande, Paraíba 58434-700, Brazil
[e] Department of Civil and Environmental Engineering, Federal University of Paraíba, Paraíba, João Pessoa 58051-900, Brazil

HIGHLIGHTS

- The relationships of biophysical variables and water and carbon fluxes for two areas in different stages of degradation.
- Gross primary production is strongly associated with water availability in the region.
- Degraded areas tend to absorb less carbon.
- The evapotranspiration rate remains high in degraded areas due to increased soil water evaporation.
- Water-use efficiency is higher in dense Caatinga than in sparse Caatinga.

GRAPHICAL ABSTRACT
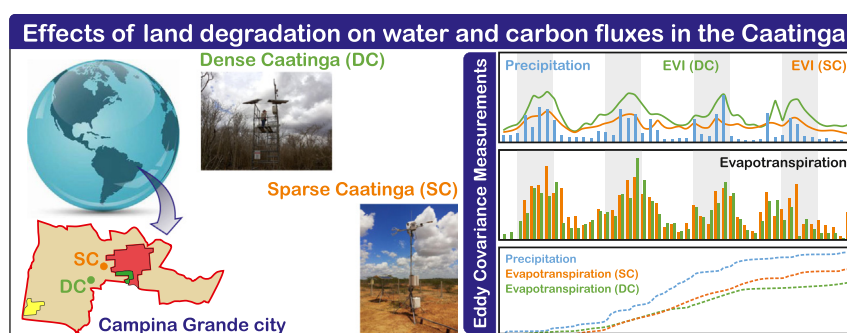
ARTICLE INFO

ABSTRACT

The Brazilian semiarid region presents a physical water scarcity and high seasonal and interannual irregularities of precipitation, known as a region with periodic droughts. This region is mainly covered by the Caatinga biome, recognized as a Seasonally Dry Tropical Forest (SDTF). Soil water availability directly impacts the ecosystem's functioning, characterized by low fertility and sparse vegetation cover during the dry season, making it a fragile ecosystem vulnerable to climatic variations. Additionally, this region has been suffering from several issues due to human activities over the centuries, which has resulted in extensive areas being severely degraded, which aggravates the impacts from climatic variations and the susceptibility to desertification. Thus, studying the soil-plant-atmosphere continuum in this region can help better understand the seasonal and annual behavior of the water and carbon fluxes. This study investigated the dynamics of water and carbon fluxes during four years (2013–2016) by using eddy covariance (EC) measurements within two areas of Caatinga (dense Caatinga (DC) and sparse Caatinga (SC)) that suffered anthropic pressures. The two study areas showed similar behavior in relation to physical parameters (air temperature, incoming radiation, vapor pressure deficit, and relative humidity), except for soil temperature. The SC area presented a surface temperature of 3 °C higher than the DC, related to their vegetation cover differences. The SC area had higher annual evapotranspiration, representing 74% of the precipitation for the DC area and 90% for the SC area. The two areas acted as a carbon sink during the study period, with the SC area showing a lower CO_2 absorption capacity. On average, the DC area absorbs 2.5 times more carbon

* Corresponding author at: Graduate Program in Engineering and Natural Resources Management, Federal University of Campina Grande, Campina Grande, Paraíba 58109-970, Brazil.
E-mail address: carlos.santos@ufcg.edu.br (C.A.C. dos Santos).

than the SC area, indicating that Caatinga deforestation affects evaporative fluxes, reducing atmospheric carbon fixation and influencing the ability to mitigate the effects of increased greenhouse gas concentrations in the atmosphere.

1. Introduction

The semiarid region of Brazil is evidenced by the scarcity of natural water reserves and seasonal and interannual irregularities of precipitation, known as a region with periodic droughts (Brasil Neto et al., 2021). Water availability in the region directly affects ecosystem functioning. This semiarid region has low fertility and scarce vegetation cover in the dry season, characterizing it as a fragile ecosystem sensitive to climatic variations (Mariano et al., 2018; Yang et al., 2019). This region has been suffering from several issues due to human activities over the centuries, resulting in extensive areas severely degraded (Antongiovanni et al., 2020), which aggravates the impacts of climatic variations and the susceptibility to desertification (Crispim et al., 2013; IPCC, 2019). In general, it has been shown that the degradation processes might begin with deforestation and the replacement of native vegetation by cultivated areas with different species sizes and/or life cycles (Antongiovanni et al., 2020). Thus, Caatinga's bush and tree vegetation is replaced by herbaceous pastures or short-cycle crops. Continued land cover transitions in this region, especially related to agriculture, lead to soil fertility loss, which affects the soil-plant-atmosphere exchanges (Perez-Marin et al., 2006).

The Caatinga biome is mainly composed of a Seasonally Dry Tropical Forest (SDTF), ranging from northwest Mexico to northern Argentina (Borges et al., 2020). A characteristic of this biome is that water availability regulates the growing season length and the phenological synchronicity, e.g., in the dry season, almost all individuals lose leaves in synchronous deciduous behavior (Silva et al., 2017; Alberton et al., 2019). Even though the Caatinga is the only biome specifically Brazilian, it is the least studied among Brazilian ecosystems and even among other tropical regions of South America (Casteletti et al., 2004; Santos et al., 2011; Koch et al., 2016). The Caatinga covers ~11% of the Brazilian territory, occupying 844,453 km^2, almost all the 980,000 km^2 of the Brazilian semiarid region, which corresponds to about 13% of the Brazilian territory (Gusmão et al., 2016). The monitoring of such a biome is quite complex due to its biotic diversity and sensitivity to climatic variations. The study of biosphere-atmosphere exchanges in this region can help better understand the energy, water, and carbon fluxes, offering support for the management and elaboration of adaptation policies related to the ecosystem responses to future climate changes.

The Caatinga has a high potential for carbon sequestration due to vegetation's high photosynthetic activity when water is available (Silva et al., 2017; Mendes et al., 2020). Gross primary production (*GPP*) occurs during photosynthesis and is strongly connected to the evapotranspiration processes (Marques et al., 2020). Quantifying the fluxes involving carbon and water exchanges allows for a better understanding of plants' survival and ecosystem's carbon cycle (Lu and Zhuang, 2010; Ito and Inatomi, 2012). It is possible to offer subsidies for assessing water scarcity and land degradation in a given area (Xie et al., 2020). These exchanges are controlled by different environmental factors, such as air temperature, vapor pressure deficit, solar radiation, and soil moisture, in addition to vegetation biological processes (e.g., leaf development and stomatal conductance) (Zha et al., 2013). Understanding the influence of these factors is crucial for assessing the effects of ecological projects and water resources management (Xie et al., 2020).

The largest source of interannual variability in the global carbon sink is drylands, covering 41% of the Earth's surface (Yao et al., 2020). These regions are expected to expand rapidly over the next century; however, the implications for variability in *GPP* remain unknown (Zheng et al., 2020; Yao et al., 2020). Thus, understanding the global carbon cycle

and predicting future climate change requires accurate estimation of the *GPP* of terrestrial vegetation (Zhang et al., 2017). Therefore, accurate *GPP* estimates are needed to understand changes in the regional and global carbon cycle, assess ecosystem health, and evaluate vegetation's response to climate change in recent years (Pei et al., 2020; You et al., 2020; Yao et al., 2020). Nevertheless, accurately reproducing interannual *GPP* variations of different biomes, including the Caatinga, remains a significant challenge, and long-term *GPP* changes are highly uncertain (Zheng et al., 2020; Mendes et al., 2020). According to Zheng et al. (2020), most *GPP* models reproduce the spatial changes but fail to represent the temporal variations. As a result, understanding the measured *GPP* interannual variations for model validation is critical because climate change and intensive human activities significantly impact vegetation productivity, causing widespread degradation in several ecosystems, particularly in drylands (You et al., 2020; Yao et al., 2020).

Few studies have been conducted on biosphere-atmosphere exchanges in Caatinga (Silva et al., 2017; Campos et al., 2019; Mendes et al., 2020; Borges et al., 2020). Additionally, there is no study about the effects of human-induced land degradation on water and carbon fluxes in contrasting soil covers on this biome. Measurements using the eddy covariance (EC) system allow to quantify the water and carbon exchanges between the biosphere and the atmosphere (Baldocchi, 2014; Chien et al., 2018; Kang et al., 2018; Coffer and Hestir, 2019; Tarin et al., 2019; Anappali et al., 2019). It is known that the study of the carbon balance in different ecosystems plays a crucial role in providing input data to large-scale models (Zhou et al., 2020). Two main studies were carried out using CO_2 flux measurements in the Caatinga. Silva et al. (2017) investigated areas of preserved Caatinga and pasture in Pernambuco, while Mendes et al. (2020) studied the seasonal variation of CO_2 exchanges in preserved Caatinga in the state of Rio Grande do Norte. Therefore, no studies have compared water and carbon fluxes in Caatinga at different land degradation stages in the same region under similar atmospheric conditions.

Vegetation restoration is an effective method for controlling desertification (Le Houérou, 2000) and an essential tool to semiarid regions' carbon cycle recovery (Zhou et al., 2020). The study of degraded areas and the vegetation's recovery process is essential for understanding their role in exchanging heat and mass at different land cover stages. Additionally, to understand how a region affected by climatic and anthropic factors (land degradation) may impact the microclimate and the desertification process (Gusmão et al., 2016). The effectiveness and accuracy of *GPP* estimates are critically important for determining the contribution of human activity and climate change (You et al., 2020). Thus, this study aimed to analyze the seasonal and annual dynamics of water and carbon fluxes in two areas of Caatinga that present varying degrees of human-induced degradation in four years (2013–2016), based on two micrometeorological towers.

The dense Caatinga (DC) area is currently defined as an area of environmental preservation and has been in the process of recovery for approximately 80 years. The sparse Caatinga (SC) area is still heavily degraded, with sparse and low vegetation. Comparing these fluxes in two nearby areas under similar meteorological conditions but with different stages of human-induced land degradation seeks precise quantification and analysis of the response of these two areas to varying degrees of anthropization and how this can impact the local microclimate.

In order to achieve the objectives, this study has been carried out based on the materials and methods described in Section 2. The results are found in Section 3, followed by the analysis and discussion

(Section 4). The article ends with the conclusions emphasizing the importance of restoring land degraded areas (Section 5).

2. Material and methods

2.1. Study area

The study was carried out in two areas of the Caatinga biome, with contrasting vegetation cover densities. The first site is a well-preserved area of the recovering Caatinga, with dense vegetation (DC). The second is a recently degraded area with sparse vegetation (SC), both located in Campina Grande, State of Paraíba, in the semiarid region of the Brazilian northeast. The two sites belong to the National Institute for Semiarid Research (INSA), where two micrometeorological towers are installed. The spatial locations of the towers can be seen in Fig. 1. The land cover map for the municipality of Campina Grande was extracted from the Brazilian Institute of Geography and Statistics (IBGE, 2020).

The DC study area has 675 ha, of which approximately 300 ha are preserved Caatinga at various stages of regeneration. The predominant vegetation is formed by sub-deciduous and deciduous forests, which lose their leaves in the drier months, composed primarily of arboreal and shrubby species. The SC area is an anthropized area, located approximately 1 km from Campina Grande city's urban area, presenting sparse vegetation with ~2 m height and a predominance of *Mimosa hostilis* trees, bare soil, and rocky outcrops (Borges et al., 2020).

The origins of degradation processes in this region are linked to climatic and edaphic conditions and land-use changes. The causes of degradation are the inappropriate use of natural resources, improper agricultural practices, and short-term macro and microeconomic development models. The removal of native cover by anthropic activities causes reduced soil fertility and an increase in soil erosion (Perez-Marin et al., 2006), suffering a gradual reduction in resilience, hindering

the recovery of these areas. The DC area has been restored for approximately 80 years, whereas the SC area is still degraded, with a slow regeneration process since 2000 (Vendruscolo et al., 2020). In both areas, the dominant soil type is litolic neosoil, characterized as shallow, reaching a maximum depth of 10 cm, moderate to imperfect drainage, excessive stony, and flat to gently undulating relief (Costa, 2019).

Based on the Köppen classification, the region's climate is semiarid, Bsh type, low latitude, and altitude (Alvares et al., 2014). The rainy season starts in February/March and lasts until July/August. According to the National Meteorology Institute (INMET, 2020), the mean annual rainfall is ~783 mm year^{-1} (1935 to 2014). The methodological flow-chart of this study is shown in Fig. 2.

2.2. Data

In the DC area, the tower was installed in January 2013 at approximately 7 m from the ground and 2 m above the vegetation's canopy. In the SC area, the tower was settled in March 2013 at the height of approximately 3 m from the ground, both instrumented with an EC sensor and micrometeorological sensors. The measurements were obtained from January 2013 to December 2016.

EC instrumentation in the towers consists of a 3D sonic anemometer (CSAT3A, Campbell Scientific, Inc., Logan, UT, USA) to measure the three components of wind speed (u_x, u_y, u_z) and a gas analyzer (EC, Campbell Scientific, Inc., Logan, UT, USA) to obtain water vapor (H_2O) and carbon dioxide (CO_2) concentrations. The measurements were performed at a high frequency (10 Hz) and stored at 30-minute intervals in a CR3000 model datalogger (Campbell Scientific, Inc., Logan, UT, USA).

A net radiometer (CNR4, Kipp & Zonen, The Netherlands) was used to obtain the shortwave radiation (downwelling and upwelling) and the longwave radiation (downwelling and upwelling) components. Temperature and relative humidity were obtained by HC2S3-L (Campbell
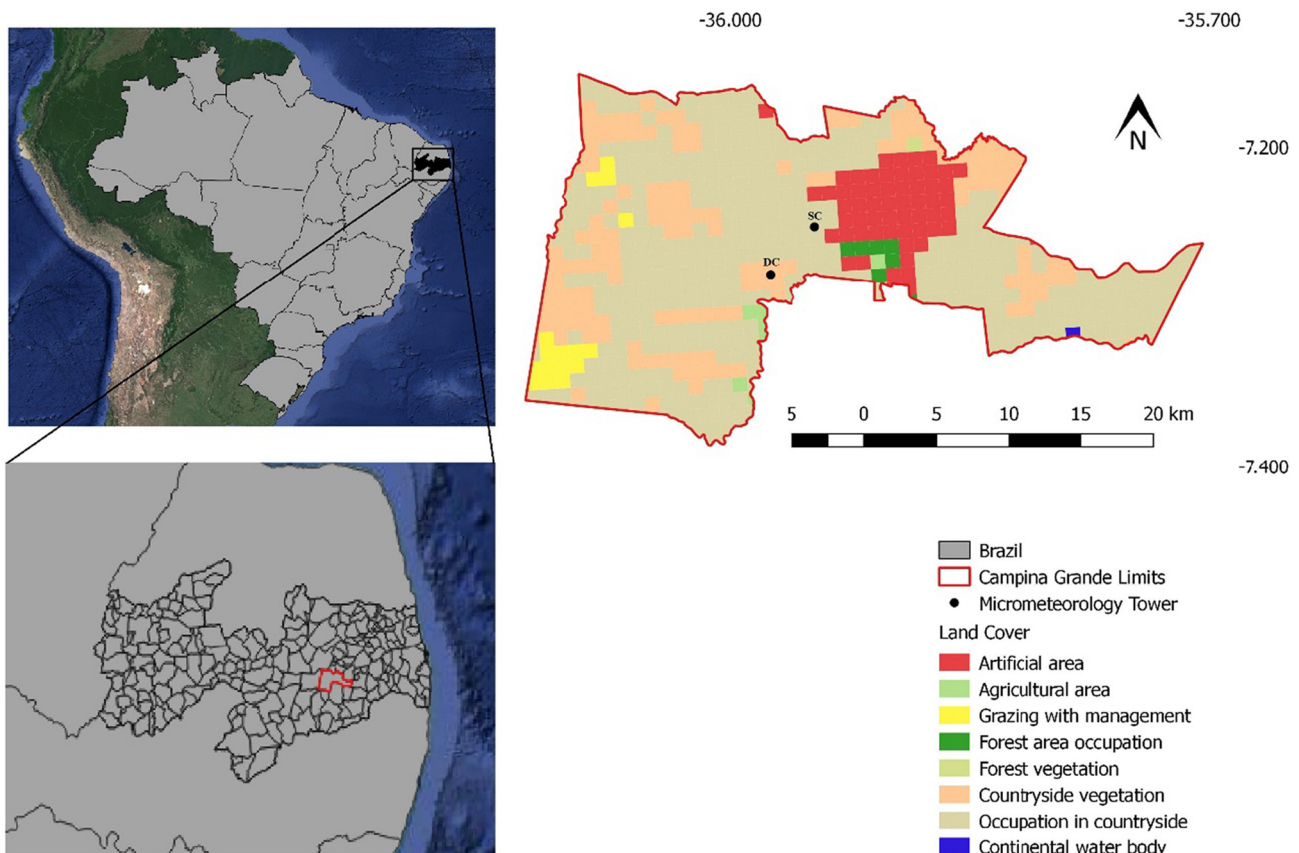

Fig. 1. Location of the study area in relation to Brazil and Paraíba (left side), land cover map for the municipality of Campina Grande, and location of the micrometeorological towers.
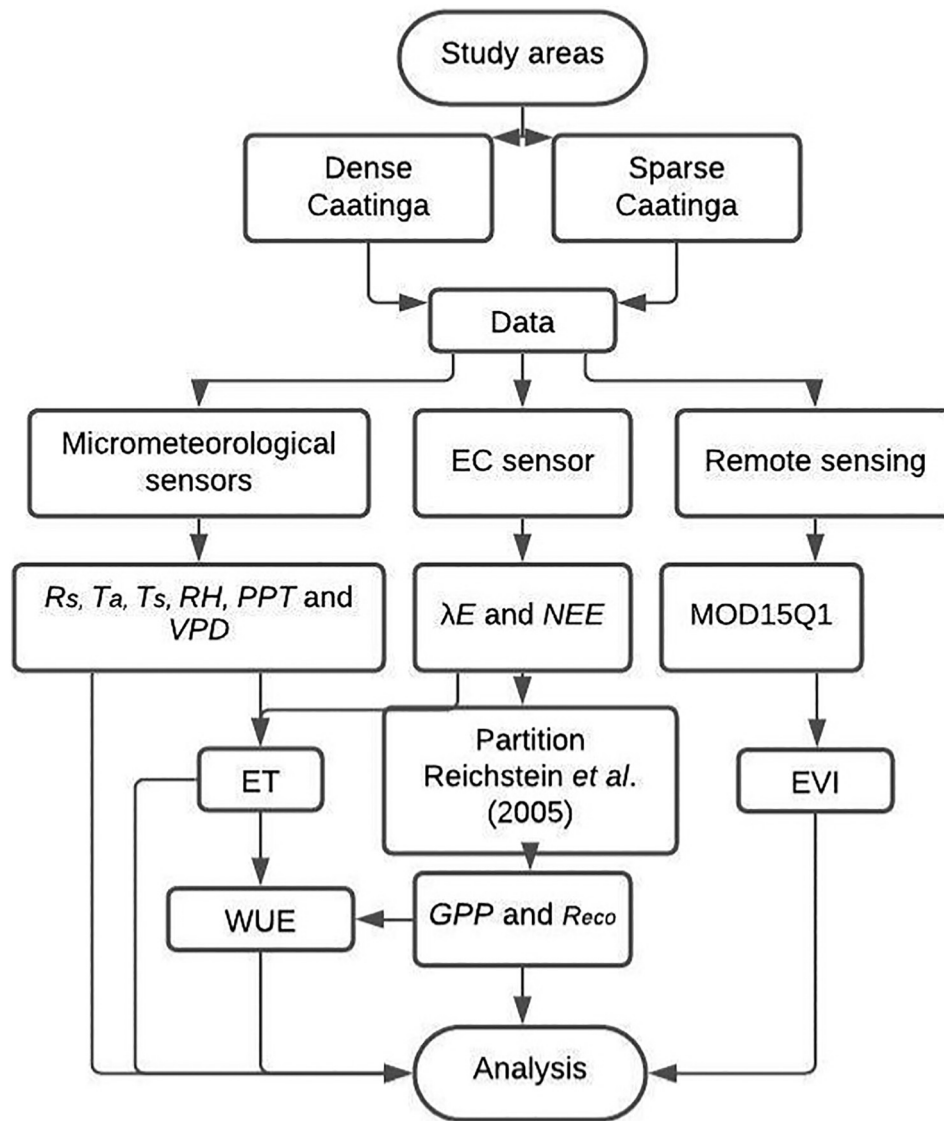
Fig. 2. Methodological flowchart of the study.

Scientific, Inc., Logan, UT, USA). Atmospheric pressure was measured by an advanced barometer (PTB110, Vaisala Corporation, Helsinki, Finland). The measurements also included two soil heat flux plates (HFP01, Campbell Scientific, Inc., Logan, UT, USA) and two soil temperature sensors (108-L, Campbell Scientific, Inc., Logan, UT, USA) installed at 2 and 10 cm depth. The measurements were performed at a low frequency (5 Hz) and stored on averages every 30 min in a datalogger model CR3000 (Campbell Scientific, Inc., Logan, UT, USA). Precipitation data was obtained from INMET. All the sensors were installed above the tree canopy, according to the manual instructions.

The enhanced vegetation index (EVI) data was obtained by remote sensing, using the product MOD13Q1 from the Moderate Resolution Imaging Spectroradiometer (MODIS) onboard the Terra satellite, providing a vegetation index value per pixel with a spatial resolution of 250 m in 16-day image compositions.

2.3. Data processing and analysis

In order to define the rainy season, it was analyzed the monthly rainfall over 25 years (1994–2019), as recorded by the INMET network. The LoggerNet software (Campbell Scientific, Inc., Logan, UT, USA) was used to obtain the latent heat flux (λE), transforming 10 Hz data into 30-

minute binary data (TOB1). The EdiRe software was used to process the high-frequency data, averaging every 30 min. Detailed information on data processing, quality control, and post-processing can be found in Campos et al. (2019).

According to the following equations, the latent heat and CO_2 fluxes were computed as a function of the covariance between the vertical wind speed (w) (m s^{-1}) and the specific humidity (q) (in kg kg^{-1}) and the CO_2 concentration (c) (μmol m^{-2} s^{-1}), respectively.

$$\lambda E = \rho \overline{w'q'} \tag{1}$$

$$FCO_2 = \rho \overline{w'c'} \tag{2}$$

where ρ corresponds to the air density (kg m^{-3}) and $\overline{w'q'}$ represents the covariance between the fluctuations of q and w, and $\overline{w'c'}$ is the covariance between w and c. The upper bars represent the product averages for the half-hour sampling interval.

In order to calculate the daily evapotranspiration (ET), the mean of the daytime measurements of the latent heat flux (λE) was used and applied in the following equation:

$$ET = 86400 \frac{\lambda E_{24h}}{\lambda \rho} \tag{3}$$

where 86,400 is the conversion from seconds to daily, ρ is the water density (1000 kg m^{-3}), and λ is the latent heat of vaporization (J kg^{-1}). For the calculation of λ (Eq. (4)), the daily average of the air temperature (T_a) (K) was used.

$$\lambda = 2.501 - 0.00236(T_a - 273.15) \times 10^6 \qquad (4)$$

CO$_2$ fluxes were partitioned to separate net ecosystem exchange (NEE) in ecosystem respiration (R$_{eco}$) and gross primary production (GPP). The fluxes partitioning method was based on Reichstein et al. (2005). For night periods, the null GPP is considered and, therefore, the NEE was estimated as follows:

$$NEE = R_{eco}, for\ night\ periods \qquad (5)$$

$$NEE = R_{eco} - GPP, for\ daytime\ periods \qquad (6)$$

NEE is positive, indicating a carbon source when CO$_2$ is transferred from the surface to the atmosphere (GPP < R$_{eco}$). NEE is negative, indicating a carbon sink when CO$_2$ is removed from the atmosphere (GPP > R$_{eco}$).

The meteorological conditions were assessed based on incoming radiation (R_s), air temperature (T_a), soil temperature at 2 cm depth (T_s), relative humidity (RH), precipitation (PPT), and vapor pressure deficit (VPD), which is the difference between the saturation vapor pressure (e_s) and the actual vapor pressure (e_a). The method used to calculate the VPD is described in Allen et al. (1998).

In order to obtain the EVI data, MOD13Q1 product pixels referring to the coordinates of the two areas were extracted with the free software R version 3.6.1 (R Core Team, 2019) through the MODISTools package, using the RStudio version 1.2.1335 interface (RStudio Team, 2019).

First, the averages for the different micrometeorological variables (daily, 24 h or daytime, 5:30–17:30 local time) were calculated. Then, to better understand the behavior of these fluxes, an analysis of daily carbon and water fluxes was performed alongside the explanatory variables. Subsequently, the annual cumulative fluxes were evaluated based on de Oliveira et al. (2018). To better understand the relationship between PPT and ET in the study area, the cumulative annual water fluxes were assessed to quantify how much PPT was used for ET. The carbon fluxes (NEE, R$_{eco}$, and GPP) were also evaluated annually to determine if the two areas of the Caatinga (DC and SC) act as a carbon sink or source during the studied period.

Finally, water-use efficiency (WUE) (g C kg^{-1} H$_2$O) was calculated as the proportion of carbon assimilation or productivity to water loss. WUE was calculated using the Beer et al. (2009) equation and is commonly used to investigate the connection between terrestrial carbon and water cycles (de Oliveira et al., 2018):

$$WUE = \frac{GPP}{ET} \qquad (7)$$

where GPP is gross primary productivity (g C m^{-2}), and ET is evapotranspiration (kg m^{-2}).

3. Results

3.1. Meteorological conditions

Fig. 3 shows the time series of the monthly averages of R_s, T_a and T_s, PPT, EVI, VPD, RH, and ET, for the two study areas (DC and SC) during four years (2013–2016). The variables showed gaps due to measurement problems. The rainy season (shaded area in the graphs) was defined from March to July, responding to ~70% of the total annual rainfall, according to the historical time series (1994–2019) recorded by the INMET network.

The incoming solar radiation (R_s) (Fig. 3a) presents low values during the rainy season (shaded area) and high values during the dry

season for both areas. During the studied period for the DC area, the minimum, maximum, and average monthly R_s were 245 W m^{-2} in June 2015 (rainy season), 413 W m^{-2} in November 2015 (dry season), and 355 W m^{-2}, respectively. The SC area showed higher values than the DC area, with the minimum, maximum, and average monthly R_s were 275 W m^{-2} in July 2015 (rainy season), 471 W m^{-2} in November 2015 (dry season), and 382 W m^{-2}, respectively.

The monthly mean T_a for the two areas was approximately 24 °C (Table 1), ranging from 26.2 °C in March 2013 to 21.5 °C in July 2015 for the DC area, and between 26.6 °C in December 2016 and 21.8 °C in July 2015 for the SC area. The two regions presented the minimum monthly average of T_a in July 2015 (Fig. 3b). The seasonal behavior of T_s (Fig. 3c) follows the same pattern as T_a, with an annual average value of 27.2 °C for DC and 30 °C for SC (Table 1), a difference of approximately 3 °C for the SC area. T_s values varied between 22.4 °C in July 2014 to 31.1 °C in March 2013 for DC and between 24.3 °C in July 2015 to 34.4 °C in November 2015 for SC (Fig. 3c). The maximum and minimum mean values of the DC area showed similar months for the two variables (T_a and T_s), with March and July showing the maximum and minimum averages, respectively. The SC area presented a minimum value in July for both variables (T_a and T_s).

The distribution of daily rainfall is shown in Fig. 3d. The year 2013 presented a more homogeneous distribution during the rainy season. 2013 also showed the highest accumulated precipitation (754.9 mm) (Table 1). The second year with the highest precipitation was 2014 (713.3 mm), which also had the majority of wet days (99 days with precipitation greater than 1.0 mm). 2015 and 2017 presented extreme precipitation events with values greater than 60 mm d^{-1} during the rainy season. Fig. 3d depicts the enhanced vegetation index (EVI) behavior to understand better how vegetation responds to precipitation events. It is possible to observe that the EVI variability follows the region's water availability, presenting maximum monthly average values (0.59 and 0.37) in the rainy season and minimum monthly values (0.11 and 0.10) in the dry season for the DC and SC areas, respectively. The average EVI (Table 1) for the DC and SC areas was 0.32 and 0.20, respectively, showing a difference of 37.5%.

The average monthly VPD values (Fig. 3e) ranged from 0.24 to 1.32 kPa for the DC area, with an average of 0.85 kPa (Table 1). The SC area varied from 0.42 to 1.31 kPa, with an average of 0.86 kPa, presenting an average similar to the DC area. The maximum values of VPD are observed during the dry season, showing an opposite behavior to relative humidity (RH) (Fig. 3f). Since VPD is a parameter that identifies the degree of dryness of the atmosphere, it helps to better comprehend ET's behavior. The monthly average values of RH (Fig. 3f) were higher than 64% for both areas, presenting greater values in the rainy season, with 76% and 75% averages for DC and SC, respectively.

The actual monthly ET (Fig. 3g) showed an average of 38.5 mm for DC and 48.2 mm for SC. The DC and SC areas showed maximum monthly values in the rainy season, reaching 125.2 mm in July 2014 in the DC area and 113.2 mm in July 2013 in the SC area. ET showed similar behavior to PPT (Fig. 3d), evidencing its strong dependence on soil moisture availability. Because of an instrumental limitation, no soil moisture data is available in the study areas.

Table 1 shows the averages for each variable during the dry and rainy periods, respectively. The variables R_s, T_a, T_s and VPD are higher in the dry season for both areas, and the opposite occurs for the variables PPT, RH and EVI, which are higher in the rainy season. 70% of PPT occurs in the rainy season. The EVI values in the rainy season had an average of 0.41 in the DC area, whereas the SC area showed an average of 0.25. The VPD values were around 0.90 in the dry period and 0.75 in the rainy period for both areas (Table 1).

3.2. Total annual evapotranspiration

The relationship between the annual cumulative PPT and ET for the DC and SC areas is shown in Fig. 4. For 2013, 2014, 2015 and 2016, the
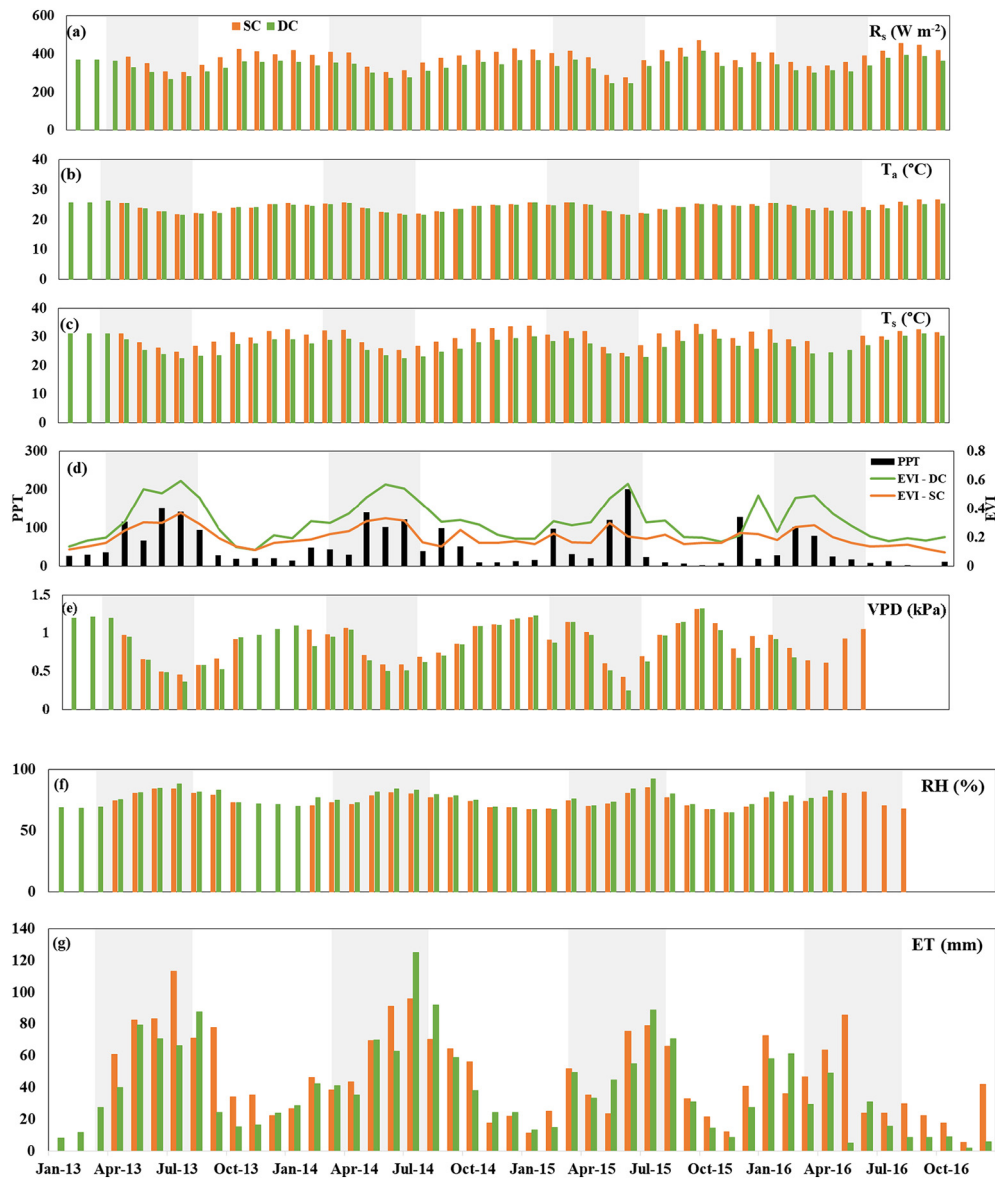
Fig. 3. Temporal distribution of environmental parameters: (a) Average monthly incident radiation (R_s) (W m^{-2}), (b) Average monthly air temperature (T_a) (°C), (c) Average monthly soil temperature (T_s) (°C), (d) Monthly precipitation (*PPT*) (mm) and monthly EVI, (e) Average monthly vapor pressure deficit (*VPD*) (kPa), (f) Average monthly relative humidity (*RH*), (g) Monthly evapotranspiration (*ET*) (mm), for the period from January 2013 to August 2016 in the two Caatinga areas (DC and SC). The shaded area indicates the rainy season.

annual *ET* represented an average of approximately 74% of the *PPT* for the DC and 90% of the *PPT* for the SC area, especially in 2014, when the annual *ET* represented 90% of the annual precipitation in both areas. 2016 was the year with the lowest annual *PPT* (440.1 mm), considerably inferior to the region's average (~783 mm year^{-1}). The same year also presented the lowest annual *ET*, 281.3 mm for DC and 468.9 mm for SC, representing an *ET*/*PPT* ratio of approximately 64% for DC. Although 2016 had the lowest annual *ET*, it was still higher than the annual *PPT*. It is worth noting that the entire study period presented annual *PPT* below the historical average as one of the most extensive and intense droughts that have occurred in northeastern Brazil (Marengo et al., 2017a,b).

The cumulative *ET* in the dry and wet periods for both areas can be seen in Table 1. The *ET* did not show significant differences between the periods, being slightly greater in the rainy season, presenting 254.8 mm for the DC area and 297.1 mm for the SC area in the rainy season. The values were 207.1 mm and 244.6 mm for the DC and SC areas during the dry period, respectively.

3.3. Carbon fluxes

Fig. 5 illustrates the monthly carbon fluxes (*GPP*, *Reco* and *NEE*) over the study period for the DC and SC areas. In the DC area (Fig. 5a, b and c), it is possible to note higher values of the *GPP* during the rainy season (shaded area of the graph), except for 2016, which presented the highest *GPP* in February (376.5 g C m^{-2}). This is likely related to the high precipitation amount in the previous month (January), reaching 127.5 mm. The monthly average of the *GPP* for the studied period was approximately 137 g C m^{-2}, with August presenting the highest monthly average. The monthly average R_{eco} was 64.6 g C m^{-2}, with a maximum of 152.9 g C m^{-2} in August 2013, with August also having the highest monthly average. The average monthly *NEE* was −72.4 g C m^{-2}, with August showing greater CO_2 absorption.

Fig. 5 also shows the monthly carbon fluxes (*GPP*, R_{eco} and *NEE*) for the SC area (Fig. 5d, e and f). Higher values of *GPP* also occurred in the rainy season, showing a monthly average of 103 g C m^{-2}, with July recording the greatest monthly average (136 g C m^{-2}). The highest

Table 1

Annual and cumulative averages of different micrometeorological and biophysical variables for the two Caatinga areas (DC and SC) (Average daily incoming solar radiation (R_s) (W m^{-2}), Average daily air temperature (T_a) (°C), Average daily soil temperature (T_s) (°C), Cumulative annual precipitation (PPT) (mm), Average daily EVI, Average daily vapor pressure deficit (VPD) (kPa), Average daily relative humidity (RH), Annual cumulative evapotranspiration (ET) (mm), Annual cumulative gross primary productivity (GPP) (g C m^{-2}), annual cumulative ecosystem respiration ($Reco$) (g C m^{-2}) and net annual cumulative ecosystem exchange (NEE) (g C m^{-2})). Annual analysis, dry and rainy seasons (2013–2016).

Variable	Annual									
	2013		2014		2015		2016		Average	
	DC	SC	DC	SC	DC	SC	DC	SC	DC	SC
R_s (W m^{-2})	334	368	327	377	339	392	345	393	336	382
T_a (°C)	24.1	23.6	23.6	23.9	24.0	24.2	24.2	24.9	24.0	24.1
T_s (°C)	27.4	28.7	26.3	29.8	27.5	30.8	27.5	30.8	27.2	30.0
PPT (mm)	754.9		713.3		558.1		440.1		616.6	
EVI (−)	0.31	0.22	0.36	0.22	0.30	0.19	0.30	0.19	0.32	0.20
VPD (kPa)	0.87	0.70	0.83	0.84	0.93	0.97	0.77	0.85	0.85	0.84
RH (%)	75.7	78.9	76.1	74.8	73.9	72.1	79.6	75.2	76.3	75.3
ET (mm)	470.4	598.4	642.9	642.6	451.7	475.9	281.3	468.9	461.6	546.5
GPP (g C m^{-2})	1130.6	1030.7	1902.6	1387.4	1499.5	1170.3	2039.1	784.3	1643.0	1093.2
$Reco$ (g C m^{-2})	737.2	770.8	893.6	797.5	722.9	769.8	744.9	589.2	774.7	731.8
NEE (g C m^{-2})	−393.4	−259.8	−1008.7	−590	−777	−400.5	−1294.2	−195.6	−868.3	−361.5
Variable	**Dry season**									
	2013		2014		2015		2016		Average	
	DC	SC	DC	SC	DC	SC	DC	SC	DC	SC
R_s (W m^{-2})	349	391	339	395	365	421	364	414	354	405
T_a (°C)	24.1	23.5	23.7	23.9	24.2	24.4	24.4	25.3	24.1	24.3
T_s (°C)	27.6	29.6	26.7	30.5	28.2	32.1	28.6	31.1	27.8	30.8
PPT (mm)	243.5		275.4		86.4		185.9		197.8	
EVI (−)	0.22	0.18	0.30	0.18	0.23	0.17	0.24	0.16	0.24	0.17
VPD (kPa)	0.92	0.72	0.90	0.92	1.07	1.09	0.73	0.93	0.91	0.92
RH (%)	74.0	77.4	74.0	72.6	69.9	69.0	79.9	72.7	74.5	72.9
ET (mm)	187.03	240.56	308.73	303.66	180.19	209.03	152.24	225	207.1	244.6
GPP (g C m^{-2})	670.09	433.78	940.9	751.86	979.68	717.73	1336.5	412.67	981.79	579.01
$Reco$ (g C m^{-2})	398.1	446.0	540.0	443.7	447.4	456.0	450.0	300.6	458.9	411.6
NEE (g C m^{-2})	−272.0	12.2	−400.9	−308.2	−532.3	−261.7	−886.5	−112.1	−522.9	−167.4
Variable	**Rainy season**									
	2013		2014		2015		2016		Average	
	DC	SC	DC	SC	DC	SC	DC	SC	DC	SC
R_s (W m^{-2})	309	336	310	353	303	352	316	358	309	350
T_a (°C)	23.9	23.4	23.6	23.6	23.8	24.0	23.7	24.1	23.8	23.8
T_s (°C)	26.4	27.5	25.8	28.8	26.5	29.0	25.6	30.0	26.1	28.8
PPT (mm)	511.4		437.9		471.7		254.2		418.8	
EVI (−)	0.43	0.28	0.45	0.29	0.39	0.21	0.37	0.22	0.41	0.25
VPD (kPa)	0.73	0.64	0.73	0.79	0.75	0.82	0.80	0.79	0.75	0.76
RH (%)	79.6	80.7	79.1	76.7	79.2	76.3	79.4	76.7	79.4	77.6
ET (mm)	283.4	340.4	334.3	338.9	271.5	265.4	130.0	243.9	254.8	297.1
GPP (g C m^{-2})	460.5	550.6	961.5	635.6	520.3	450.5	704.5	372.2	661.7	502.2
$Reco$ (g C m^{-2})	339.1	308.3	353.6	353.8	275.5	310.5	296.9	288.7	316.3	315.3
NEE (g C m^{-2})	−121.4	−242.4	−607.9	−281.8	−244.8	−140.0	−407.6	−83.5	−345.4	−186.9

monthly value occurred in July 2014, reaching approximately 184 g C m^{-2}. R_{eco} monthly average was 69.2 g C m^{-2}, with the highest monthly average in August. The average NEE was −33.7 g C m^{-2}, with May showing higher CO_2 absorption (−96 g C m^{-2}).

It was noted that the DC area absorbed an additional 34 g C m^{-2} monthly in relation to the SC area, which is equivalent to 33% more carbon absorbed. Regarding R_{eco}, the two areas showed approximate values, with a slight difference of 2 g C m^{-2} more for the DC area. Consequently, the NEE of the DC area was greater than the SC area, with a difference of approximately −39 g C m^{-2} monthly. This difference exceeds the monthly average of NEE in the SC area, which is only −33.7 g C m^{-2}.

Fig. 6 presents the annual cumulative carbon fluxes (GPP, R_{eco} and NEE) in the DC area for 2013, 2014, 2015, and 2016, showing that 2016 had the highest cumulative GPP (2039.1 g C m^{-2}). As expected, it also showed the highest NEE (−1294.2 g C m^{-2}), with the total carbon being fixed approximately two times greater than the carbon released by respiration (744.9 g C m^{-2}). In 2014 and 2015, total fixed carbon values also were higher than carbon released via respiration.

2013 presented the lowest cumulative GPP (1130.6 g C m^{-2}). Even then, the total fixed carbon was 53% higher than the carbon released. The DC area absorbed more carbon than it emitted for the entire period, with an average fixed total carbon (NEE) 1.1 times greater than the lost carbon (R_{eco}).

Fig. 7 shows the annual carbon fluxes (GPP, $Reco$ and NEE) in the SC area for the studied period (2013–2016). 2016 presents the cumulative values for eight months, from January to August, due to instrument record issues. The total cumulative carbon fluxes in Fig. 7 show that 2014 had the highest cumulative GPP (1387.4 g C m^{-2}). Consequently, the highest NEE (−590 g C m^{-2}), with the total carbon fixed 74% higher than the carbon released by respiration. 2014 and 2015 showed total fixed carbon values 51% higher than the carbon released. In 2013 and 2016, the total carbon fixed was 33% higher than the carbon lost via respiration. Thus, for the entire period, the area absorbed more carbon than it emitted.

Only the complete two-year dataset of the SC area (2014 and 2015) and four years of the DC area (2013–2016) were used to compare the annual totals for the two areas. The annual average difference of the
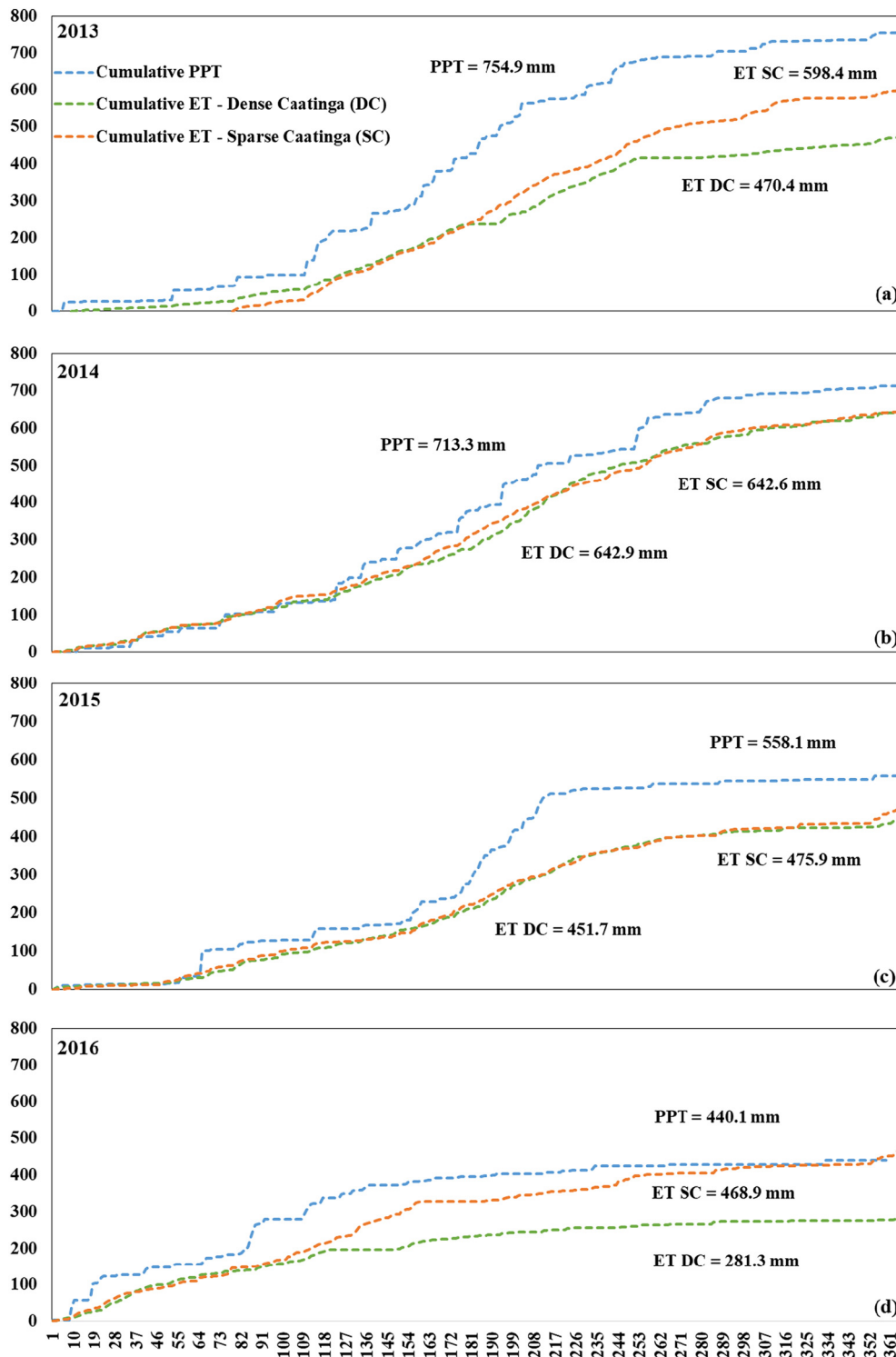
Fig. 4. Cumulative precipitation (*PPT*) (mm) and cumulative evapotranspiration (*ET*) (mm) for the studied period (2013, 2014, 2015, and 2016) for the DC and SC areas.

GPP was 364.2 g C m^{-2} more for the DC area. R_{eco} presented similar values of close to 780 g C m^{-2} for both areas. Consequently, the DC area absorbed more carbon, showing a *NEE* annual average of about −868 g C m^{-2}. In contrast, the SC area absorbed about −495 g C m^{-2}, corresponding to 56% of the DC area's total carbon absorption.

In addition, it was evaluated the seasonal (dry and rainy) carbon fluxes (Table 1). It was observed that *GPP* and *Reco* presented greater cumulative values in the dry period than in the rainy period for the two areas. Consequently, showing lower *NEE* does not necessarily mean that higher carbon absorption values are found in the dry period.

Higher values occur in the rainy period when analyzing the monthly carbon fluxes (Fig. 4). However, as the rainy period (five months) is smaller than the dry period (seven months), the total values may be higher in the dry period.

3.4. Water-use efficiency (WUE)

The *WUE* annual mean was 5.2 and 2.7 g C kg^{-1} H$_2$O for the DC and SC areas, respectively. Both areas had low *WUE* values in the rainy season (Fig. 8) due to the higher water consumption. The SC area showed
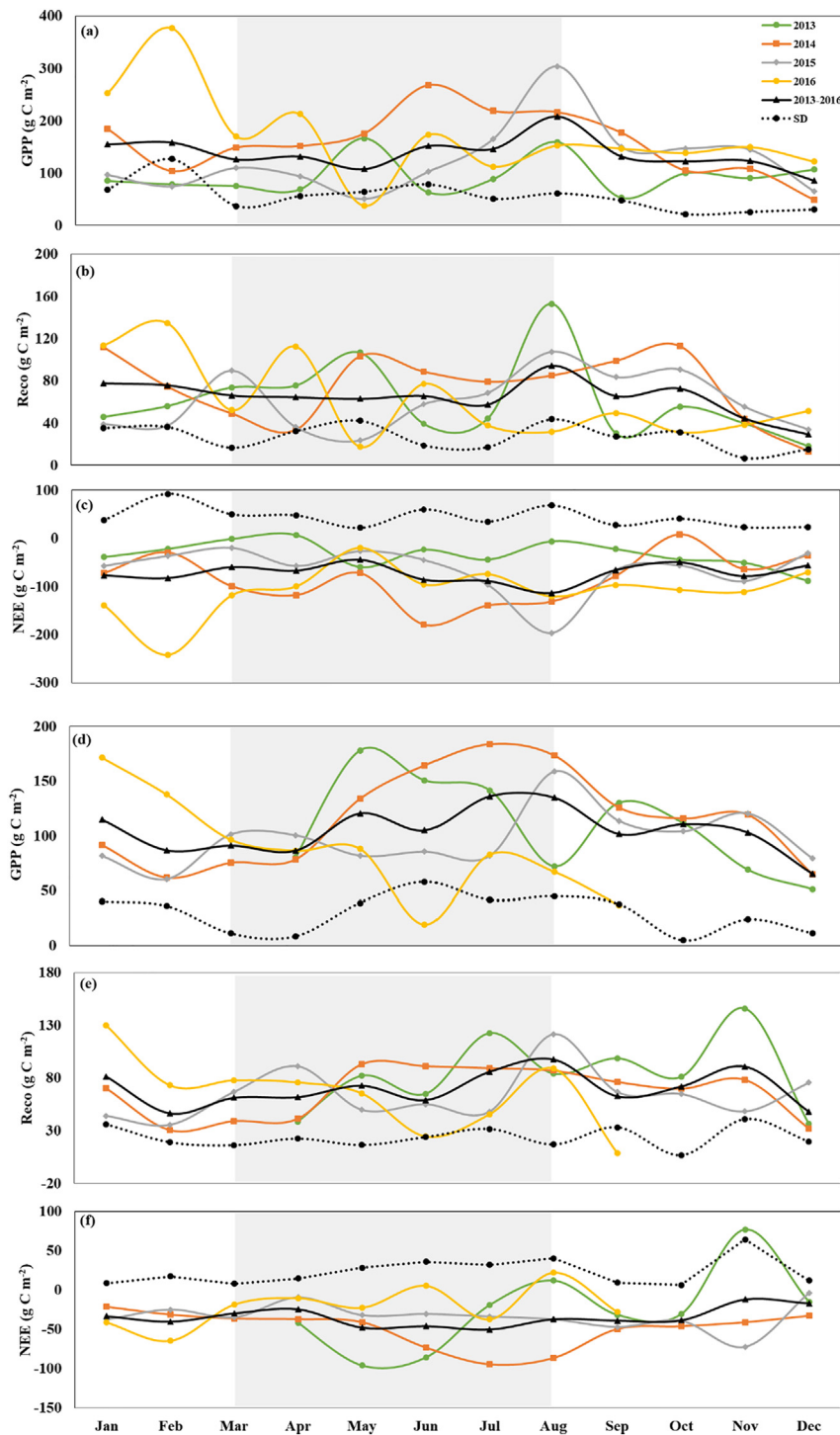
Fig. 5. Monthly values of gross primary productivity (*GPP*), ecosystem respiration (*Reco*), and net ecosystem exchange (*NEE*), all fluxes in g C m^{-2}, and standard deviation (SD) for the DC area (a, b and c) and the SC area (d, e and f).

lower values of *WUE* in relation to the DC area. This likely occurs due to the rapid growth of grasses in this area, indicating a high water loss rate. Another factor contributing to the low *WUE* in the SC area is related to high soil water loss. This occurs because the SC area has a higher percentage of bare soil, which favors water loss through evaporation. Fig. 8c shows the annual *WUE*, evidencing that the SC *WUE* was lower than DC in all years, with 2016 being significantly higher for the DC area. The averages *WUE* for the rainy season were 3.3 and 1.9 g C kg^{-1}

H$_2$O for the DC and SC areas, whereas the dry season's averages were 6.6 and 3.3 g C kg^{-1} H$_2$O, respectively.

The Caatinga's *WUE* values proved to be high in relation to studies in other areas (de Oliveira et al., 2018) due to the plants' photorespiration mechanism present in the Caatinga biome (C4 and CAM). C4 and CAM plants are common in arid and semiarid regions. These plants have adaptations for carbon fixation and water loss due to water stress, which leads them to lose less water through transpiration (via stomatal
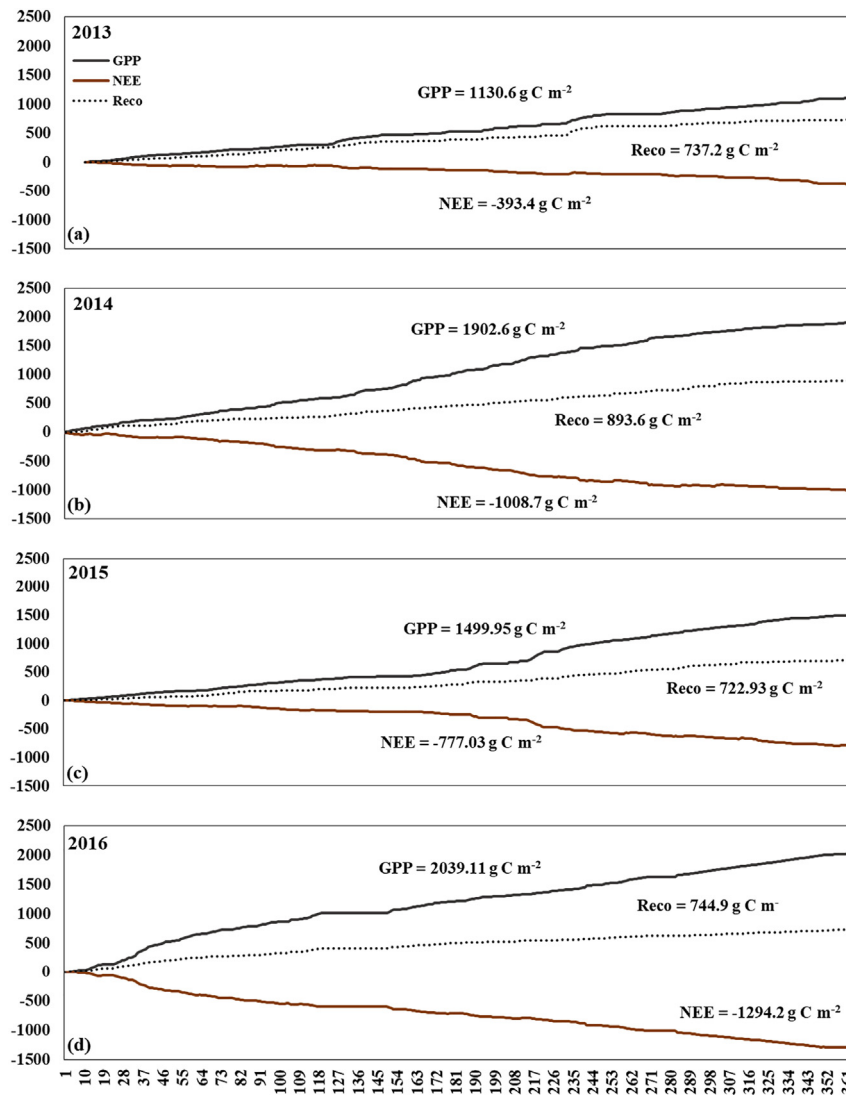
Fig. 6. Cumulative gross primary productivity (*GPP*), ecosystem respiration (*Reco*), and net ecosystem exchange (*NEE*) for the studied period (2013, 2014, 2015, and 2016) for the dense Caatinga (DC) area.

closure) (Hatfiel and Dold, 2019), therefore presenting higher water-use efficiency.

4. Discussion

The meteorological conditions observed during the experiment showed that the region was under drought conditions during most of the study period, with an annual rainfall below the region's historical average. The causes of the drought were due to the positive anomalies influence on the sea surface temperatures (SST) of the Equatorial Pacific and Tropical North Atlantic Oceans, with the development of an El Niño event, particularly in 2015, and contributing to the displacement of the Intertropical Convergence Zone (ITCZ) to the north of the equator, causing a reduction in rainfall (Marengo et al., 2017a,b).

It is observed in Fig. 3a that the maximum values of R_s are identified in the dry season, when the lowest cloud cover is notorious, causing less interference in the incoming solar radiation. The highest values of R_s were found in the SC area. The T_a data was similar for both sites, presenting average values of approximately 24 °C. From Fig. 3b, it is observed that after the rainy season in 2016, the T_a values for the SC area differ from the values of the DC area, presenting an average increase of approximately 1.2 °C, with a slight variation in its behavior at the

end of the studied period. This variation can be explained by the increase of R_s in the same period. The high temperatures during 2016 are likely an effect of the drought that occurred in that year. As it can be seen in Table 1, 2016 presented the lowest annual precipitation in relation to the other studied years. The seasonal variation of the daily average T_a was approximately 10 °C, with maximum values observed in the dry season, in which the clear sky provides a greater surface absorption of R_s, as clouds reduce the amount of incoming solar energy at the Earth's surface due to its high reflectivity (Querino et al., 2011).

T_s in the SC area is, on average 3 °C higher than in the DC area. This is explained because SC is under severe land degradation and has a higher percentage of bare soil, absorbing more energy, thereby increasing T_s. Colaizzi et al. (2016) explain that in soils under this condition, the soil heat flux (G) can correspond to up to 50% of the net radiation (R_n) due to the considerable variation in the R_s incoming into the soil.

The temporal distribution of rainfall had a significant impact on the EVI (Fig. 3d). It is evidenced by the high seasonality of the vegetation cover during the studied period, with a greater variation for the DC area, as it is an area with more vegetation cover. The DC area reached the maximum daily value (0.74) during the rainy season and the lowest (0.06) during the dry season, showing Caatinga's high seasonality. The phenology of vegetation tends to respond quickly to rainfall events.
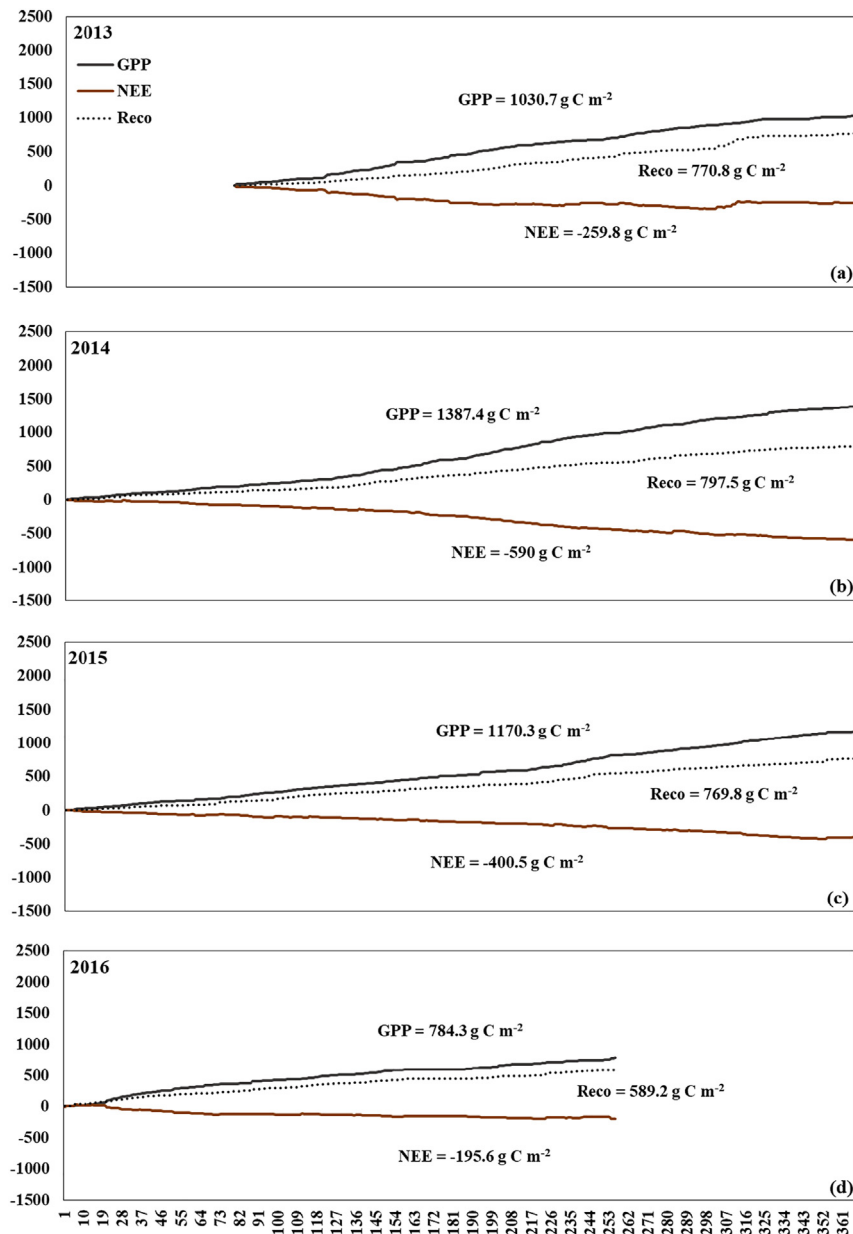
Fig. 7. Cumulative primary gross productivity (*GPP*), ecosystem respiration (*Reco*), and net ecosystem exchange (*NEE*) for the studied period (2013, 2014, 2015, and 2016) for the sparse Caatinga (SC) area.

Thus, during the rainy season, it is expected that vegetation, especially deciduous species, strengthens its metabolic activities, as noted by Barbosa and Kumar (2016) and da Silva et al. (2017).

Differences in vegetation coverage were observed between the two studied areas for the rainy season, with an average variation of 0.16, corresponding to approximately 39%. In the dry period, when the senescence process occurs, the DC area still presents higher values than the SC area due to the presence of some semideciduous species (Marques et al., 2020). The *VPD* and *RH* values showed opposite behaviors for the two areas, as shown in Fig. 3e and f. It is evidenced that, as the *VPD* increases, the *RH* decreases and, consequently, decreases the *ET* (Fig. 3g). This behavior is because the *VPD* indicates the degree of dryness of the atmosphere; thus, there is a direct relationship between these three parameters. Therefore, since it is dependent on the vapor pressure gradient between the evaporating surface and the air in the rainy periods, it is usual for the atmosphere to be frequently with high moisture content, significantly reducing the *VPD* (Rodrigues et al., 2011).

As expected, *ET* reached its maximum in the rainy season for both areas. In the dry season, the leaf senescence response to water stress reduces the *ET* rates (Marques et al., 2020). The behavior of *ET* in the Caatinga was consistent with previous studies in the Brazilian semiarid region, such as Silva et al. (2017) and Marques et al. (2020).

The SC area presented the highest annual cumulative *ET* values, as shown in Table 1 and Fig. 4. One of the hypotheses for this behavior would be greater soil evaporation, as it is an area with a large percentage of bare soil (Graf et al., 2020), in addition to the fast growth of grasses, favoring transpiration. Also, the plants are younger, tending to have a higher *ET* than the older plants in the DC area. Therefore, adding the two mechanisms (evaporation + transpiration) of water loss, the SC area becomes responsible for the greatest water transfer to the atmosphere. As the DC area has more covered soil (higher EVI), *ET* may be lower in relation to water loss reduction through evaporation. Also, DC plants have mechanisms for reducing water loss by the transpiration process (Freitas et al., 2006; Menezes et al., 2013).
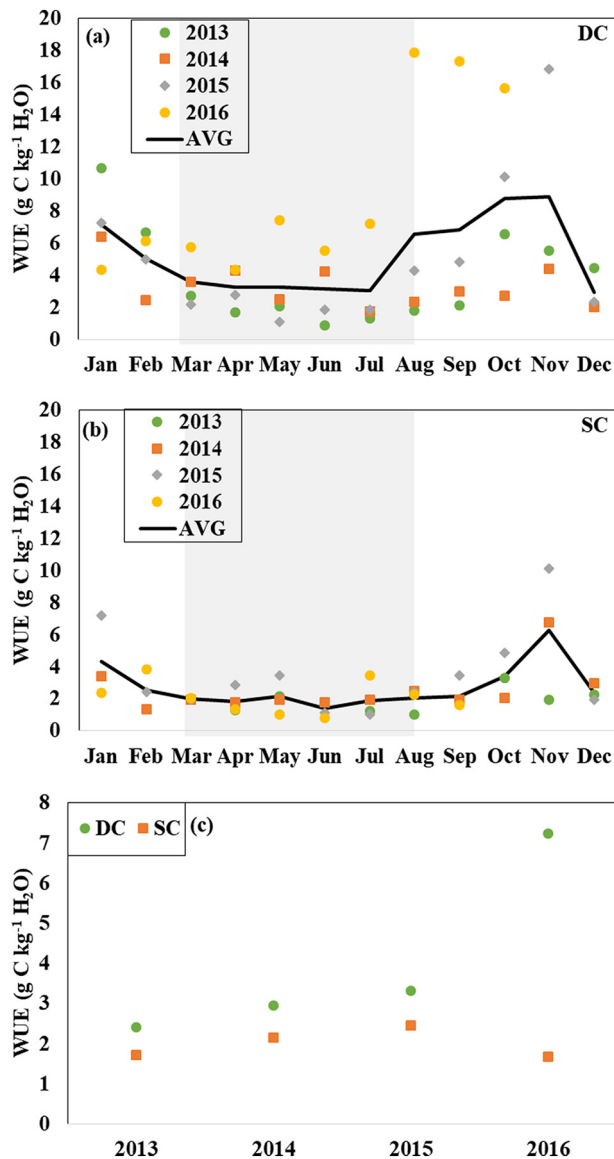
Fig. 8. Monthly water-use efficiency (WUE) (g C kg^{-1} H$_2$O) for DC (a) and SC (b) and annual for both areas (c) from 2013 to 2016. The shaded area represents the rainy season.

A strong relationship between *GPP* (Fig. 5) and EVI (Fig. 3d) was observed during the study period. Xu and Baldocchi (2004), Gitelson et al. (2014), and de Oliveira et al. (2018) found similar results, considering different vegetation types. It is important to note that Mendes et al. (2020) also observed a strong relationship between EVI and *GPP* in the Caatinga area. The relationship between *GPP* and EVI is observed with greater intensity in the DC area (the area with the highest *GPP*).

In both areas, it was observed that *GPP* rates exceeded R_{eco}, acting as a carbon sink. A similar result was found by Rotenberg and Yakir (2010) when studying the contribution of semiarid forests to the climate system. In the DC area, 2016 was the year that showed *GPP* 2.7 times higher than R_{eco}. The highest R_{eco} values were also recorded in the same year, maybe related to the EVI increase. The average *GPP*/R_{eco} ratio for the DC region was 2.2. In the SC area, the average is approximately 1.5, and the highest *GPP*/R_{eco} ratio (i.e., 1.7) was verified in 2014. These results agree with those found in several semiarid regions worldwide and described by Baldocchi et al. (2018), presenting a full review of the inter-annual variability of the net and gross ecosystem carbon fluxes from different ecosystems.

In the dry season, the values of carbon fluxes tend to decrease considerably (Fig. 5). This is due to the occurrence of leaf senescence and

the fact that photosynthetic activities are restricted to a few semideciduous plant species, as previously stated. Mendes et al. (2020) explain that trees are likely to suffer from the decrease in soil water content during the dry season, leading to reduced stomatal conductance and leaf transpiration, limiting the assimilation of CO$_2$, further reducing the net photosynthesis. R_{eco} values for Caatinga are considered below average compared to other studies in different ecosystems (Baldocchi et al., 2018). This is because the Caatinga biome (shorter trees and grass predominance) has lower carbon stocks than humid regions (taller trees and vigorous understory canopies) (Plaza et al., 2018, Baldocchi et al., 2018). In addition, plants tend to maintain respiration at baseline levels during water scarcity events, presenting low autotrophic respiration rates (Santos et al., 2014).

Table 1 shows that 2016, despite having the highest *NEE*, also had the lowest *PPT* and *ET* for the DC area. Baldocchi (2019) explains that 57% of *NEE*'s interannual variability is responsible for biological effects, and the residual (43%) due to climatic conditions. In this regard, it is hypothesized that these unexpected increases in *NEE* in 2016 may be highly related to vegetation's phenology, with minor influences of the physical parameters.

From Fig. 5, it is observed high respiration rates, mainly in the SC area. These maximum values are likely related to the "Birch effect" (Birch, 1958; Jarvis et al., 2007), where rainfall in semiarid ecosystems can induce many pulses of CO$_2$, with the size of the pulse depending on the degree of previous photodegradation and decreasing with time, after successive rain events (Huxman et al., 2004; Ma et al., 2012). Higher rates of R_{eco} in the DC area might be related to the roots production and the proportional contributions of younger soil respiration, in addition to the decomposition of organic matter.

Table 1 shows that the DC area had the highest CO$_2$ assimilation rate than the SC area (up to 2.5 times). The R_{eco}/*GPP* ratio is 46% for DC and 66% for SC, i.e., the SC area returns 20% more carbon than was absorbed by the *GPP* to the atmosphere than the DC area. Baldocchi (2019) explains that the growing season's duration substantially impacts the cumulative sum of assimilated carbon. As a result, a degraded area with low vegetation cover and a shorter growing season tends to absorb less CO$_2$, as observed by Rotenberg and Yakir (2010). However, during the study period, it was observed a high interannual variability. Several studies have shown that the ecosystem-atmosphere carbon fluxes suffer varying degrees of interannual variability due to climatic, ecological, and physiological factors, as Baldocchi et al. (2018) stated. Thus, longer datasets are necessary to detect and better explain the causes of this variability.

One of the aspirations of this study was to assess the interannual variability of the water and carbon fluxes in the Caatinga biome under different human-induced land degradation stages. It is worth highlighting a severe drought event in the area during the study period, showing precipitation below the historical average. Similar analyses in wetter periods, including evaluations of soil water content and vegetation's stomatal conductance, would be interesting to understand these interactions better.

Even considering that only four years were used in this study, the results obtained here can support management policies and sustainable practices that minimize the effects of climate variations, contributing to adaptation strategies for this particular and important biome in South America. Recent studies indicate a trend in reducing native vegetation areas, resulting in increased land degradation, triggered by replacing natural land cover with pasture and agricultural lands (Antongiovanni et al., 2020). Thus, according to Strassburg et al. (2020), the effects of ecosystem degradation and climate change have resulted in significant interest in ecosystem restoration at the national, regional, and global levels. The conservation of the remaining natural ecosystems is the most critical focus for preserving biodiversity.

Understanding how different types of degradation in such a unique environment, given the fact that the Caatinga is the only biome that exists solely within the Brazilian territory, and the consequent impact in

the fluxes of water and carbon has international relevance, for example, to establish comparisons on how different biomes are affected by regimes of disturbance, as it can be seen, e.g., in Miao et al. (2009), da Silva et al. (2018), McNicol et al. (2018), Sagar et al. (2019), Brando et al. (2019), Yao et al. (2020) and Antongiovanni et al. (2020). These results are also important to understand how different soil-vegetation-atmosphere feedbacks may exacerbate the future expected warmer and drier conditions in this region.

The findings of this study have a significant impact on our understanding of soil-plant-atmosphere continuum exchanges in the Caatinga biome and the environmental consequences of land degradation in drylands. As a result, emphasize the urgency of conservation actions by providing general guidelines for planning, management, and monitoring efforts that may mitigate the effects of disturbance.

5. Conclusions

This study investigated the effect of the Caatinga biome degradation on water and carbon exchanges in the Brazilian semiarid region. This is the first study examining and relating carbon fluxes in areas with different human-induced land degradation stages in this biome. It was observed that the sparse Caatinga had annual evapotranspiration higher than the dense Caatinga, corresponding to an average of 90% of the total annual precipitation, while the dense Caatinga used about 74%. Consequently, the Caatinga deforestation contributes to the evapotranspiration intensification (by soil water loss) and the reduction of the potential for fixing atmospheric carbon, reducing the capability of this STDF to mitigate the effects of the increasing concentration of greenhouse gases in the atmosphere. Additionally, the two areas acted as a carbon sink, absorbing an average of 50% and 34% of the total fixed carbon for the dense and sparse Caatinga areas, respectively. As expected, deforestation of the Caatinga biome reduces the ecosystem's capacity to absorb CO_2 and modifies the microclimate, impacting the local and regional carbon budget. These findings provide a better understanding of how different types of degradation in this unique region may affect the expected warmer and drier conditions of the Caatinga in the years to come.

CRediT authorship contribution statement

Michele L. de Oliveira: Conceptualization, Methodology, Software, Data curation, Writing – original draft, Visualization, Investigation, Writing – review & editing. **Carlos A.C. dos Santos:** Conceptualization, Methodology, Software, Data curation, Writing – original draft, Visualization, Investigation, Supervision, Writing – review & editing. **Gabriel de Oliveira:** Conceptualization, Methodology, Software, Visualization, Investigation, Supervision, Writing – review & editing. **Aldrin M. Perez-Marin:** Writing – review & editing. **Celso A.G. Santos:** Writing – review & editing.

Declaration of competing interest

The authors declare that they have no known competing financial interests or personal relationships that could have appeared to influence the work reported in this paper.

Acknowledgments

References

Alberton, B., Torres, R.S., Silva, T.S.F., da Rocha, H.R., Moura, M.S., Morellato, L.P.C., 2019. Leafing patterns and drivers across seasonally dry tropical communities. Remote Sens. 11, 2267. https://doi.org/10.3390/rs11192267.

Allen, R.G., Pereira, L.S., Raes, D., Smith, M., 1998. Crop Evapotranspiration: Guidelines for Computing Crop Water Requirements. United Nations FAO, Irrigation and Drainage Paper 56. FAO, Rome, Italy.

Alvares, C.A., Stape, J.L., Sentelhas, P.C., Gonçalves, J.L.M., Sparovek, G., 2014. Köppen's climate classification map for Brazil. Meteorol. Z. 8, 711–728. https://doi.org/10.1127/0941-2948/2013/0507.

Anappali, S.S., Fisher, D.K., Reddy, K.N., Krutz, J.L., Pinnameni, S.R., Sui, R., 2019. Quantifying water and CO_2 fluxes and water use efficiencies across irrigated C_3 and C_4 crops in a humid climate. Sci. Total Environ. 663, 338–350. https://doi.org/10.1016/j.scitotenv.2018.12.471.

Antongiovanni, M., Venticinque, E.M., Matsumoto, M., Fonseca, C.R., 2020. Chronic anthropogenic disturbance on Caatinga dry forest fragments. J. Appl. Ecol. 57, 2064–2074. https://doi.org/10.1111/1365-2664.13686.11/1365-2664.13686.

Baldocchi, D., 2014. Measuring fluxes of trace gases and energy between ecosystems and the atmosphere - the state and future of the eddy covariance method. Glob. Chang. Biol. 20 (12), 3600–3609. https://doi.org/10.1111/gcb.12649.

Baldocchi, D.D., 2019. How eddy covariance flux measurements have contributed to our understanding of Global Change Biology. Glob. Chang. Biol. 26, 242–260. https://doi.org/10.1111/gcb.14807.

Baldocchi, D., Chu, H., Reichstein, M., 2018. Inter-annual variability of net and gross ecosystem carbon fluxes: a review. Agric. For. Meteorol. 249, 520–533. https://doi.org/10.1016/j.agrformet.2017.05.015.

Barbosa, H.A., Kumar, T.V.L., 2016. Influence of rainfall variability on the vegetation dynamics over Northeastern Brazil. J. Arid Environ. 124, 377–387. https://doi.org/10.1016/j.jaridenv.2015.08.015.

Beer, C., Ciais, P., Reichstein, M., Baldocchi, D., Law, B.E., Papale, D., Soussana, J.F., Ammann, C., Buchmann, N., Frank, D., Gianelle, D., 2009. Temporal and among-site variability of inherent water use efficiency at the ecosystem level. Glob. Biogeochem.Cycles 23, 1–13. https://doi.org/10.1029/2008GB003233.

Birch, H.F., 1958. Further aspects of humus decomposition. Nature 182 (4643), 1172. https://doi.org/10.1038/1821172a0.

Borges, C.K., dos Santos, C.A.C., Carneiro, R.G., Silva, L.L., de Oliveira, G., Mariano, D., Silva, M.T., da Silva, B.B., Bezerra, B.G., Perez-Marin, A.M., Medeiros, S.S., 2020. Seasonal variation of surface radiation and energy balances over two contrasting areas of the seasonally dry tropical forest (Caatinga) in the Brazilian semi-arid. Environ. Monit. Assess. 192, 524. https://doi.org/10.1007/s10661-020-08484-y.

Brando, P.M., Silvério, D., Maracahipes-Santos, L., Oliveira-Santos, C., Levick, S.R., Coe, M.T., Migliavacca, M., Balch, J.K., Macedo, M.N., Nepstad, D.C., Maracahipes, L., 2019. Prolonged tropical forest degradation due to compounding disturbances: implications for CO2 and H_2O fluxes. Glob. Chang. Biol. 25 (9), 2855–2868.

Brasil Neto, R.M., Santos, C.A.G., Costa Silva, J.F.C.B., Silva, R.M., Santos, C.A.C., Mishra, M., 2021. Evaluation of the TRMM product for monitoring drought over Paraíba State, northeastern Brazil: a trend analysis. Sci. Rep. 11, 1097. https://doi.org/10.1038/s41598-020-80026-5.

Campos, S., Mendes, K.R., da Silva, L.L., Mutti, P.R., Medeiros, S.S., Amorim, L.B., dos Santos, C.A.C., Perez-Marin, A.M., Ramos, T.M., Marques, T.V., Lucio, P.S., Costa, G.B., e Silva, C.M.S., Bezerra, B.G., 2019. Closure and partitioning of the energy balance in a preserved area of a Brazilian seasonally dry tropical forest. Agric. For. Meteorol. 271, 398–412. https://doi.org/10.1016/j.agrformet.2019.03.018.

Casteletti, C.H.M., Silva, J.M.C., Taberelli, M., Santos, A.M.M., 2004. Quanto ainda resta da caatinga? Uma estimativa preliminar. Biodiversidade da caatinga: áreas e ações prioritárias para conservação. MMA.

Chien, H., Zhong, Y., Yang, K., Cheng, H., 2018. Diurnal variability of CO2 flux at coastal zone of Taiwan based on eddy covariance observation. Cont. Shelf Res. 162, 27–38. https://doi.org/10.1016/j.csr.2018.04.006.

Coffer, M.M., Hestir, E.L., 2019. Variability in trends and indicators of CO2 exchange across Arctic wetlands. J. Geophys. Res. Biogeosci. 124, 1248–1264. https://doi.org/10.1029/2018JG004775.

Colaizzi, P.D., Evett, S.R., Agam, N., Schwartz, R.C., Kustas, W.P., Cosh, M.H., Mckee, L., 2016. Soil heat flux calculation for sunlit and shaded surfaces under row crops: 2. Model test. Agric. For. Meteorol. 216, 129–140. https://doi.org/10.1016/j.agrformet.2015.10.009.

Costa, C.R.G., 2019. Dinâmica temporal do efluxo de co2 e produção de glomalina em área de caatinga sob neossolo litólico. Dissertação. UFPB.

Crispim, A.B., Melo, C.C.F., Almeida, I.C.S., Oliveira, L.S., 2013. Bases introdutórias sobre degradação ambiental no semiárido brasileiro. III SERNNE.

da Silva, P.F., Lima, J.R.S., Antonino, A.C.D., Souza, R., de Souza, E.S., Silva, J.R.I., Alves, E.M., 2017. Seasonal patterns of carbon dioxide, water and energy fluxes over the Caatinga and grassland in the semi-arid region of Brazil. J. Arid Environ. 147, 71–82. https://doi.org/10.1016/j.jaridenv.2017.09.003.

da Silva, J.M.C., Leal, I.R., Tabarelli, M. (Eds.), 2018. Caatinga: The Largest Tropical Dry Forest Region in South America. Springer.

de Oliveira, G., Brunsell, N.A., Sutherlin, C.E., Crews, T.E., DeHann, L.R., 2018. Energy, water and carbon exchange over a perennial Kernza wheatgrass crop. Agric. For. Meteorol. 249, 120–137. https://doi.org/10.1016/j.agrformet.2017.11.022.

Freitas, P.S.L., Mantovani, E.C., Sediyama, G.C., Costa, L.C., 2006. Influência da cobertura de resíduos de culturas nas fases da evaporação direta da água do solo. Revista Brasileira de Engenharia Agrícola e Ambiental 10, 104–111.

Gitelson, A.A., Peng, Y., Arkebauer, T.J., Schepers, J., 2014. Relationships between gross primary production, green LAI, and canopy chlorophyll content in maize: implications for remote sensing of primary production. Remote Sens. Environ. 144, 65–72. https://doi.org/10.1016/j.rse.2014.01.004.

Graf, A., et al., 2020. Altered energy partitioning across terrestrial ecosystems in the European drought year 2018. Philos. Trans. R. Soc. B 375, 20190524. https://doi.org/10.1098/rstb.2019.0524.

Gusmão, L.F.P., Queiroz, L., Bravo, F., Juncá, F.A., Oliveira, R.P., Baseia, I.G., 2016. CAATINGA: Diversidade na adversidade do semiárido brasileiro. MCTIC.

Hatfiel, J.L., Dold, C., 2019. Water-use efficiency: advances and challenges in a changing climate. Front. Plant Sci. 10, 103. https://doi.org/10.3389/fpls.2019.00103.

Huxman, T.E., Snyder, K.A., Tissue, D., Leffler, A.J., Ogle, K., Pockman, W.T., Schwinning, S., 2004. Precipitation pulses and carbon fluxes in semiarid and arid ecosystems. Oecologia 141 (2), 254–268. https://doi.org/10.1007/s00442-004-1682-4.

IBGE, 2020. Instituto Brasileiro de Geografia e Estatística. Disponível em:. https://www.ibge.gov.br/geociencias/informacoes-ambientais/cobertura-e-uso-da-terra/15833-uso-da-terra.html?=&t=downloads. (Accessed November 2020).

INMET, 2020. Instituto Nacional de Meteorologia. Disponível em:. https://portal.inmet.gov.br/. (Accessed November 2020).

IPCC, 2019. Climate Change and Land: An IPCC Special Report on Climate Change, Desertification, Land Degradation, Sustainable Land Management, Food Security, and Greenhouse Gas Fluxes in Terrestrial Ecosystems [P.R. Shukla, J. Skea, E. Calvo Buendia, V. Masson-Delmotte, H.-O. Pörtner, D. C. Roberts, P. Zhai, R. Slade, S. Connors, R. van Diemen, M. Ferrat, E. Haughey, S. Luz, S. Neogi, M. Pathak, J. Petzold, J. Portugal Pereira, P. Vyas, E. Huntley, K. Kissick, M. Belkacemi, J. Malley, (eds.)]. (In press).

Ito, A., Inatomi, M., 2012. Water-use efficiency of the terrestrial biosphere: a model analysis focusing on interactions between the global carbon and water cycles. J. Hydrometeorol. 13, 681–694. https://doi.org/10.1175/JHM-D-10-05034.1.

Jarvis, P., Rey, A., Petsikos, C., Wingate, L., Rayment, M., Pereira, J., Valentini, R., 2007. Drying and wetting of Mediterranean soils stimulates decomposition and carbon dioxide emission: the "Birch effect". Tree Physiol. 27, 929–940. https://doi.org/10.1093/treephys/27.7.929.

Kang, X., Yan, L., Zhang, X., Li, Y., Tian, D., Peng, C., Wu, H., Wang, J., Zhong, L., 2018. Modeling gross primary production of a typical coastal wetland in China using MODIS time series and CO2 eddy flux tower data. Remote Sens. 10 (5), 708. https://doi.org/10.3390/rs10050708.

Koch, R., Almeida-Cortez, J.S., Kleinschmit, B., 2016. Revealing areas of high nature conservation importance in a seasonally dry tropical forest in Brazil: combination of modelled plant diversity hot spots and threat patterns. J. Nat. Conserv., 35 https://doi.org/10.1016/j.jnc.2016.11.004.

Le Houérou, H.N., 2000. Restoration and rehabilitation of arid and semiarid Mediterranean ecosystems in North Africa and West Asia: a review. Arid Soil Res. Rehabil. 14 (1), 3–14. https://doi.org/10.1080/089030600263139.

Lu, X., Zhuang, Q., 2010. Evaluating evapotranspiration and water-use efficiency of terrestrial ecosystems in the conterminous United States using MODIS and AmeriFlux data. Remote Sens. Environ. 114, 1924–1939. https://doi.org/10.1016/j.rse.2010.04.001.

Ma, S., Baldocchi, D.D., Hatala, J.A., Detto, M., Curiel, Y.J., 2012. Are rain-induced ecosystem respiration pulses enhanced by legacies of antecedent photodegradation in semi-arid environments? Agric. For. Meteorol. 154–155, 203–213. https://doi.org/10.1016/j.agrformet.2011.11.007.

Marengo, J.A., Alves, L.M., Alvala, R.C.S., Cunha, A.P., Brito, S., Moraes, O.L.L., 2017a. Climatic characteristics of the 2010–2016 drought in the semiarid Northeast Brazil region. Ann. Braz. Acad. Sci. https://doi.org/10.1590/0001-3765201720170206.

Marengo, J.A., Torres, R.R., Alves, L.M., 2017b. Drought in Northeast-Brazil - past, present, and future. Theor. Appl. Climatol. 129, 1189–1200. https://doi.org/10.1007/s00704.016-1840-8.

Mariano, D.A., dos Santos, C.A.C., Wardlow, B.D., Anderson, M.C., Schiltmeyer, A.V., Tadesse, T., Svoboda, M.D., 2018. Use of remote sensing indicators to assess the effects of drought and human-induced land degradation on ecosystem health in Northeastern Brazil. Remote Sens. Environ. 213, 129–143. https://doi.org/10.1016/j.rse.2018.04.048.

Marques, T.V., Mendes, K., Mutti, P., Medeiros, S., Silva, L., Perez-Marin, A.M., Campos, S., Lúcio, P.S., Lima, K., dos Reis, J., Ramos, T.M., da Silva, D.F., Oliveira, C.P., Costa, G.B., Antonino, A.C.D., Menezes, R.S.C., e Silva, C.M.S., Bezerra, B., 2020. Environmental and biophysical controls of evapotranspiration from Seasonally Dry Tropical Forest (Caatinga) in the Brazilian Semiarid. Agric. For. Meteorol., 287 https://doi.org/10.1016/j.agrformet.2020.107957.

McNicol, I.M., Ryan, C.M., Mitchard, E.T., 2018. Carbon losses from deforestation and widespread degradation offset by extensive growth in African woodlands. Nat. Commun. 9 (1), 1–11.

Mendes, K.R., Campos, S., da Silva, L.L., Mutti, P.R., Ferreira, R.R., Medeiros, S.S., Perez-Marin, A.M., Marques, T.V., Ramos, T.M., Vieira, M.M.L., Oliveira, C.P., Gonçalves, W.A., Costa, G.B., Antonino, A.C.D., Menezes, R.S.C., Bezerra, B.G., Silva, C.M.S., 2020. Seasonal variation in net ecosystem CO2 exchange of a Brazilian seasonally dry tropical forest. Sci. Rep. 10, 9454. https://doi.org/10.1038/s41598-020-66415-w.

Menezes, J.A.L., Santos, T.E.M., Montenegro, A.A.A., Silva, J.R.L., 2013. Comportamento temporal da umidade do solo sob Caatinga e solo descoberto na Bacia Experimental do Jatobá, Pernambuco. Water Resour. Irrig. Manag. 2, 45–51.

Miao, H., Chen, S., Chen, J., Zhang, W., Zhang, P., Wei, L., Han, X., Lin, G., 2009. Cultivation and grazing altered evapotranspiration and dynamics in Inner Mongolia steppes. Agric. For. Meteorol. 149 (11), 1810–1819.

Pei, Y., Dong, J., Zhang, Y., Yang, J., Zhang, Y., Jiang, C., Xiao, X., 2020. Performance of four state-of-the-art GPP products (VPM, MOD17, BESS and PML) for grasslands in drought years. Ecol. Inform. 56, 101052. https://doi.org/10.1016/j.ecoinf.2020.101052.

Perez-Marin, A.M., Menezes, R.S.C., Silva, E.D., Sampaio, E.V.S., 2006. Effects of Gliricidia sepium on soil nutrients, microclimate and maize yield in an agroforestry system in semi-arid Paraiba, Brazil. Rev. Bras. Ciênc. Solo 30, 555–564. https://doi.org/10.1590/S0100-06832006000300015.

Plaza, C., Zaccone, C., Sawicka, K., Méndez, A.M., Tarquis, A., Gascó, G., Heuvelink, G.B.M., Schuur, E.A.G., Maestre, F.T., 2018. Soil resources and element stocks in drylands to face global issues. Sci. Rep. 8, 13788. https://doi.org/10.1038/s41598-018-32229-0.

Querino, C.A.S., Moura, M.A.L., Querino, J.K.A.S., Radow, C.V., Filho, A.O.M., 2011. Study of the global solar radiation and the internal and external transmissivity index in a mangrove forest in Alagoas - Brazil. Rev. Bras. Meteorol. 26 (2). https://doi.org/10.1590/S0102-77862011000200005.

R Core Team, 2019. R: A Language and Environment for Statistical Computing. R Foundation for Statistical Computing, Vienna, Austria.

Reichstein, M., Falge, E., Baldocchi, D., Papale, D., Aubinet, M., Berbigier, P., Bernhofer, C., Buchmann, M., Gilmaninov, T., Granier, A., 2005. On the separation of net ecosystem exchange into assimilation and ecosystem respiration: review and improved algorithm. Glob. Change Biol. 11 (9), 1424–1439. https://doi.org/10.1111/j.1365-2486.2005.001002.x.

Rodrigues, A., Pita, G., Mateus, J., Kurz-Besson, C., Casquilho, M., Cerasoli, S., Gomes, A., Pereira, J., 2011. Eight years of continuous carbon fluxes measurements in a Portuguese eucalypt stand under two main events: drought and felling. Agric. For. Meteorol. 151 (4), 493–507. https://doi.org/10.1016/j.agrformet.2010.12.007.

Rotenberg, E., Yakir, D., 2010. Contribution of semi-arid forests to the climate system. Science 327, 451–454. https://doi.org/10.1126/science.1179998.

RStudio Team, 2019. RStudio: Integrated Development Environment for R. RStudio, Inc., Boston, MA.

Sagar, R., Li, G.Y., Singh, J.S., Wan, S., 2019. Carbon fluxes and species diversity in grazed and fenced typical steppe grassland of Inner Mongolia, China. J. Plant Ecol. 12 (1), 10–22.

Santos, J.C., Leal, I.R., Cortez-Almeida, J.S., Fernandes, G.W., Tabarelli, M., 2011. Caatinga: the scientific negligence experienced by a dry tropical forest. Trop. Conserv. Sci. 4 (3), 276–286. https://doi.org/10.1177/194008291100400306.

Santos, M.G., Oliveira, M.T., Figueiredo, K.V., Falcão, H.M., Arruda, E.C.P., Almeida-Cortez, J., Sampaio, E.V.S.B., Ometto, J.P.H.B., Menezes, R.S.C., Oliveira, A.F.M., Pompelli, M.F., Antonino, A.C.D., 2014. Caatinga, the Brazilian dry tropical forest: can it tolerate climate changes? Theor. Exp. Plant Physiol. 26, 83–99. https://doi.org/10.1007/s40626-014-0008-0.

Silva, P.F., Lima, J.R.S., Antonino, A.C.D., Souza, R., Souza, E.D., Silva, J.R.L., Alves, E.M., 2017. Seasonal patterns of carbon dioxide, water and energy fluxes over the Caatinga and grassland in the semi-arid region of Brazil. J. Arid Environ. 147, 71–82. https://doi.org/10.1016/j.jaridenv.2017.09.003.

Strassburg, B.B.N., Iribarrem, A., Beyer, H.L., et al., 2020. Global priority areas for ecosystem restoration. Nature 586, 724–729. https://doi.org/10.1038/s41586-020-2784-9.

Tarin, T., Nolan, H.R., Medlyn, B.E., Cleverly, J., Eamus, D., 2019. Water-use efficiency in a semi-arid woodland with high rainfall variability. Glob. Chang. Biol. 26, 498–508. https://doi.org/10.1111/gcb.14866.

Vendruscolo, J., Perez-Marin, A.M., Felix, E.S., Ferreira, K.R., Cavalheiro, W.C.S., Fernandes, I.M., 2020. Monitoring desertification in semiarid Brazil: using the Desertification Degree Index (DDI). Land Degrad. Dev., 1–15 https://doi.org/10.1002/ldr.3740.

Xie, S., Mo, X., Hu, S., Liu, S., 2020. Contributions of climate change, elevated atmospheric CO2 and human activities to ET and GPP trends in the Three-North Region of China. Agric. For. Meteorol. 295, 108183. https://doi.org/10.1016/j.agrformet.2020.108183.

Xu, L., Baldocchi, D.D., 2004. Seasonal variation in carbon dioxide exchange over a Mediterranean annual grassland in California. Agric. For. Meteorol. 123, 79–96. https://doi.org/10.1016/j.agrformet.2003.10.004.

Yang, Z., Zhang, Q., Hao, X., Yue, P., 2019. Changes in evapotranspiration over global semi-arid regions 1984–2013. J. Geophys. Res. Atmos. 124 (6), 2946–2963. https://doi.org/10.1029/2018JD029533.

Yao, J., Liu, H., Huang, J., et al., 2020. Accelerated dryland expansion regulates future variability in dryland gross primary production. Nat. Commun. 11, 1665. https://doi.org/10.1038/s41467-020-15515-2.

You, N., Meng, J., Zhu, L., Jiang, S., Zhu, l., Li, F., Kuo, L., 2020. Isolating the impacts of land use/cover change and climate change on the GPP in the Heihe River Basin of China. J. Geophys. Res. Biogeosci. 125, e2020JG005734. https://doi.org/10.1029/2020JG005734.

Zha, T., Li, C., Kellomäki, S., Peltola, H., Wang, K.Y., Zhang, Y., 2013. Controls of evapotranspiration and CO2 fluxes from scots pine by surface conductance and abiotic factors. PLoS One 8 (7), e69027. https://doi.org/10.1371/journal.pone.0069027.

Zhang, Y., Xiao, X., Wu, X., et al., 2017. A global moderate resolution dataset of gross primary production of vegetation for 2000–2016. Sci. Data 4, 170165. https://doi.org/10.1038/sdata.2017.165.

Zheng, Y., Shen, R., Wang, Y., Li, X., Liu, S., Liang, S., Chen, J.M., Ju, W., Zhang, L., Yuan, W., 2020. Improved estimate of global gross primary production for reproducing its long-term variation, 1982–2017. Earth Syst. Sci. Data 12, 2725–2746. https://doi.org/10.5194/essd-12-2725-2020.

Zhou, J., Li, X., Gao, Y., He, M., Wang, M., Wang, Y., Zhao, L., Li, Y., 2020. Carbon fluxes response of an artificial sand-binding vegetation system to rainfall variation during the growing season in the Tengger Desert. J. Environ. Manag. 266, 110556. https://doi.org/10.1016/j.jenvman.2020.110556.